

transform. All of the computations reported in this article were performed with use of the computing resources of the National Center for Atmospheric Research which is supported by the National Science Foundation. Finally, this research has been supported by the National Science Foundation Grant No. 77-10093ATM.

^(a)Currently on leave from the Mathematics Department, University of Colorado, Boulder, Colo. 80309.

¹E. N. Lorenz, *J. Atmos. Sci.* **20**, 130 (1963).

²D. Ruelle and J. Takens, *Commun. Math. Phys.* **20**, 167 (1971).

³J. B. McLaughlin and P. C. Martin, *Phys. Rev. A* **12**, 186 (1975).

⁴J. H. Curry, *Commun. Math. Phys.* **60**, 193 (1978).

⁵J. P. Gollub and S. V. Benson, *Phys. Rev. Lett.* **41**, 978 (1978).

⁶J. Marsden and M. McCracken, *The Hopf Bifurcation and Its Applications*, Applied Mathematical Sciences Series, Vol. 19 (Springer, Berlin, 1976).

⁷B. Saltzman, *J. Atmos. Sci.* **19**, 329 (1962).

⁸S. Newhouse, D. Ruelle, and F. Takens, *Commun. Math. Phys.* **64**, 35 (1978).

⁹S. Newhouse, private communication (1979).

Study of Driven Lower-Hybrid Waves in the Alcator Tokamak using CO₂-Laser Scattering

C. M. Surko^(a) and R. E. Slusher^(a)

Bell Laboratories, Murray Hill, New Jersey 07974

and

J. J. Schuss, R. R. Parker, I. H. Hutchinson, D. Overskei, and L. S. Scaturro

Massachusetts Institute of Technology, Cambridge, Massachusetts 02139

(Received 12 April 1979)

The wavelengths, amplitudes, frequencies, and spatial distributions of driven lower-hybrid wave fluctuations are studied in the Alcator tokamak with use of CO₂-laser scattering. It is found that for incident microwave power densities from 0.4 to 4.5 kW/cm² the wave amplitudes are nearly independent of the relative phase of the electric fields at the exciting waveguides. The waves are not localized in resonant cones and they have frequency widths of from 0.5 to 6 MHz.

A potentially important method for heating tokamak plasmas involves the generation of lower-hybrid waves which propagate to the center of the plasma and then deposit energy into the ions and electrons. Until now, however, it has not been possible to study directly lower-hybrid waves in a hot tokamak plasma. In this Letter we report a study of driven lower-hybrid waves in the Alcator tokamak using the small-angle scattering¹ of CO₂ laser radiation. The results indicate that the wave amplitudes and spectra are nearly independent of the relative phase of the exciting fields of the two-waveguide launching structure; the waves are distributed in broad annular regions of the minor cross section of the torus and are not confined to resonant cones.

The frequency ν_0 of the incident microwaves is 2.45 GHz. A two-port waveguide array (described elsewhere)² launches the lower-hybrid waves with total incident microwave powers of up to 90 kW (power densities up to 4.5 kW/cm²). The rel-

ative phase φ of the fields at the waveguides is adjustable from 0° to 360°. The position of the face of the waveguide, x_w , is adjustable from the plasma chamber wall, 12.5 cm from the magnetic axis, to the limiter radius, a , at 10 cm. The CO₂ laser beam, which is located 90° around the major direction of the torus from the waveguide, is parallel to the major axis of symmetry of the torus and can traverse the minor cross section at major radii located +8, +4, 0, and -4 cm from the magnetic axis. We denote these positions by x/a of 0.8, 0.4, 0, and -0.4, respectively. The scattering angles are adjusted to measure the wavelengths λ_{\perp} of waves propagating nearly perpendicular to the incident laser beam¹ and to the toroidal magnetic field. For each λ_{\perp} , the range of wave vectors $|\vec{k}_{\perp}|$ (equal to $2\pi/\lambda_{\perp}$) sampled is constant and equal to 10 cm⁻¹ half width at half maximum. Depending on the position in the plasma, \vec{k}_{\perp} is a mixture of radial and poloidal wave-vector components. Scattered

light is heterodyne detected with a local oscillator (LO) beam split off from the incident beam.¹ The LO beam intersects the incident beam as it passes through the plasma so that the alignment of the LO and scattered radiation necessary for heterodyne detection is guaranteed. The Ge:Cu detector, designed by Airborne Instrument Laboratories, has a high quantum efficiency near 0.1 at 2.5 GHz.

The D₂ plasma duration was 120 ms, the toroidal magnetic field was 60 kG, and the plasma currents were near 150 kA. The microwave power lasted 20 ms starting 60 ms after the beginning of the discharge. The scattered signals were dependent on plasma density; however, the signals, if present, were reasonably constant throughout the heating pulse.

Shown in Fig. 1 is the dependence of the mean squared amplitude of the scattered signal as a function of both the incident microwave power and the relative phase of the waveguides. The laser beam was at x/a of +0.4, λ_{\perp} was 0.07 cm, x_w was 12.5 cm, and the signals were integrated over a 1-MHz band centered at ν_0 . The frequency and wave-vector spectrum of the scattered signal did not vary significantly over the microwave power range shown in Fig. 1. Thus the signal is proportional to the square of the electron density fluctuation \tilde{n}_e^2 and is a direct measure of the relative conversion efficiency of microwave power into lower-hybrid waves. The chord-averaged density was 1.1 to 1.2×10^{14} cm⁻³ for the solid

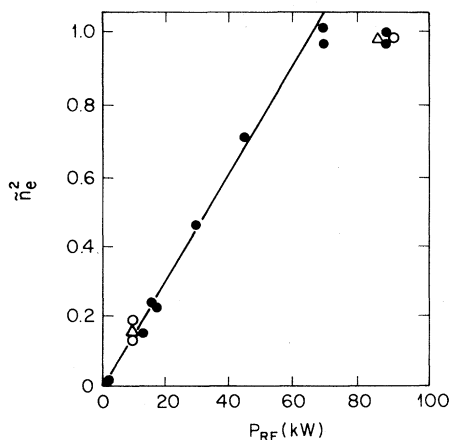


FIG. 1. The wave amplitude \tilde{n}_e^2 as a function of incident microwave power P_{rf} . The solid and open circles represent data with the relative phase φ at the waveguides of 180° and the triangles represent data with φ equal to 0° .

circles and 0.6 to 0.8×10^{14} cm⁻³ for the open symbols, and the amplitudes \tilde{n}_e^2 for these density ranges were normalized at 90 kW. The parallel index of refraction N_{\parallel} (equal to $c/\nu_0\lambda_{\parallel}$) for these lower-hybrid waves is calculated from the electrostatic dispersion relation to be 5 for the open symbols and 4 for the solid symbols. The experimental wave-vector resolution introduces an uncertainty in N_{\parallel} of ± 0.5 . Up to 70 kW, \tilde{n}_e^2 is a linear function of incident power as predicted by linear theory. However, the saturation between 70 and 90 kW and the lack of dependence of \tilde{n}_e^2 on φ (comparing the open circles and triangles in Fig. 1) disagrees with this theory.^{3,4} As the waveguide was moved into the plasma, \tilde{n}_e^2 was found to change with φ but only in proportion to the net microwave power transmitted into the torus. For example, when x_w was decreased to 11 cm, \tilde{n}_e^2 decreased from its values at x_w of 12.5 cm by ratios of 0.6 and 0.42 for φ equal to 180° and 0° , respectively, while the transmitted power decreased by corresponding ratios of 0.64 and 0.36. For this experiment N_{\parallel} was 4 and linear theory³ would have predicted changes in \tilde{n}_e^2 of more than a factor of 2 with a reversal of φ at constant net microwave power as compared with the observed factor of 1 ± 0.2 .

Shown in Figs. 2 and 3 is the density dependence of the scattered signal in a 1-MHz bandwidth about ν_0 for the laser beam at x/a of +0.8 and +0.4. The unit of chord-averaged density, \bar{n} , is 10^{14} cm⁻³. The different symbols correspond to data taken during individual operating days. Preliminary data from vertical scans along the incident beam indicate that the signal arises from a region within ± 5 cm of the midplane of the torus and therefore the observed fluctuations have predominantly radial wave vectors.

If the lower-hybrid waves excited by the microwave array propagated in well-defined resonant cones as observed previously in some plasma devices,⁵ the width of these cones at the laser beam would be about 1 mm which is also the radius of laser beam. A light-scattering signal would then require the plasma density and current to be adjusted precisely for one of the widely spaced resonant cones and laser beam to coincide. We therefore have evidence that the waves are not confined to resonant cones, since the scattered signal is approximately constant throughout the microwave pulse and the density dependence of the signal is relatively smooth (Figs. 2 and 3). At x/a of 0 and -0.4 the data are similar to those shown in Fig. 3(b). These data also indicate a

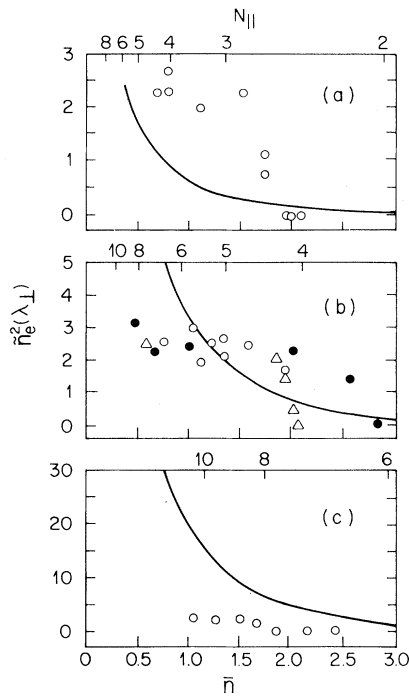


FIG. 2. The dependence of $\tilde{n}_e^2(\lambda_\perp)$ on chord-averaged density \bar{n} for λ_\perp of (a) 0.12 cm, (b) 0.07 cm, and (c) 0.04 cm, with the laser beam at $x/a = 0.8$.

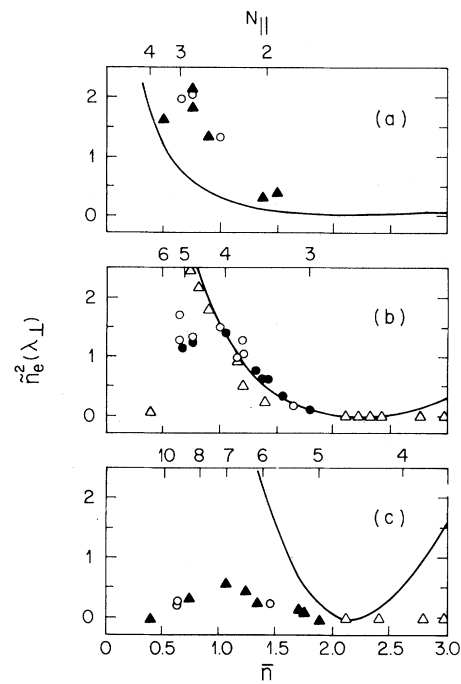


FIG. 3. The dependence of $\tilde{n}_e^2(\lambda_\perp)$ on chord-averaged density \bar{n} for λ_\perp of (a) 0.12 cm, (b) 0.07 cm, and (c) 0.04 cm, with the laser beam at $x/a = 0.4$.

broad spatial distribution of the fluctuations, and the data at x/a of zero indicates the existence of appreciable poloidal wave-vector components.

The scattered signal has a frequency width $\Delta\nu$ which increases linearly with density from 0.5 to 6 MHz and which is independent of microwave power from 7 to 90 kW. As \bar{n} increases above $0.7 \times 10^{14} \text{ cm}^{-3}$ the frequency spectrum becomes asymmetric. The peak of the frequency distribution shifts down from ν_0 by as much as 1 to 2 MHz for \bar{n} greater than $1 \times 10^{14} \text{ cm}^{-3}$. Preliminary data show that $\Delta\nu$ increases as x/a decreases from 0.8 to 0.4 and that $\Delta\nu$ in hydrogen plasmas is larger than in deuterium plasmas by nearly 40% at constant \bar{n} and 20% at constant N_{\parallel} .

The expected dependence of $\tilde{n}_e^2(\lambda_\perp)$ on \bar{n} is shown by the solid curves in Figs. 2 and 3, under the assumption that the waves have a uniform power density as a function of N_{\parallel} and propagate without damping. It is also assumed that the scattering is produced near the midplane of the torus, and warm-plasma corrections are included. A factor of $1/\bar{n}$ is included for the solid curves to account for the observed increase of $\Delta\nu$ with \bar{n} . The upper scale for each value of λ_\perp denotes the values of N_{\parallel} as determined from the electro-

static lower-hybrid dispersion relation, and thus scanning \bar{n} scans the N_{\parallel} spectrum. The amplitude of the calculation was normalized only at \bar{n} of $1 \times 10^{14} \text{ cm}^{-3}$ and λ_\perp of 0.07 cm at x/a of 0.4. In Fig. 3 the zeros in the solid curves as \bar{n} increases are due to a cancellation of the inertial motion of the electrons along the magnetic field and the polarization drift.

A comparison of the calculations and measurements in Figs. 2 and 3 shows that the data are consistent with a broad spectrum of waves with N_{\parallel} 's from 2.5 to 6 with decreasing intensity as N_{\parallel} increases above 3. The wave amplitudes decrease more rapidly than expected above \bar{n} of $2 \times 10^{14} \text{ cm}^{-3}$. If chord-averaging effects are included, the zeros in the solid curves in Fig. 3 become only minima and this effect is even more striking. This decrease in wave amplitudes with increasing \bar{n} is evidence of either increased attenuation or decreased launching efficiency. Finally, a comparison of Figs. 2(b) and 3(c) indicates that the higher- N_{\parallel} waves are attenuated as they propagate into the plasma which is qualitatively consistent with electron heating observed between \bar{n} of $(1.0 \text{ and } 1.2) \times 10^{14} \text{ cm}^{-3}$ and enhanced neutron emission between $(1.3 \text{ and } 2) \times 10^{14} \text{ cm}^{-3}$.²

At mean densities less than $1 \times 10^{14} \text{ cm}^{-3}$ the observed fluctuation levels $\tilde{n}_e(\lambda_{\perp})/\bar{n}$ in a 1-MHz bandwidth about ν_0 and in a wave-vector interval of 20 cm^{-1} were near 10^{-4} . When integrated over frequency, wave-vector, and plasma cross section these levels are consistent with the conversion of an appreciable fraction (0.01 to 1.0) of the incident microwave power into lower hybrid waves. In previous, less sensitive, experiments on the ATC tokamak⁵ a limit of less than 10^{-3} was set for a similar measurement of $\tilde{n}_e(\lambda_{\perp})/\bar{n}$. This limit is less than the level predicted for resonant cone propagation and indicates the possibility of spatial frequency or wave-vector broadening of lower-hybrid waves during ATC experiments.

There is a high level of low-frequency density fluctuations which peak near the radius of the limiter for $\bar{n} \approx 0.5 \times 10^{14} \text{ cm}^{-3}$.¹ That the lower-hybrid waves are not localized in resonance cones is consistent with their being scattered by these low-frequency fluctuations^{7,8} by angles which are expected to be⁸ of the order of 90° . A portion of the frequency width of the lower-hybrid waves may also be due to the low-frequency fluctuations; however, the expected widths are 1 to 2 MHz as compared with the observed widths of up to 6 MHz. The explanation of the lack of dependence of the waves on φ and the asymmetry of the frequency spectra is not yet clear.

This study of lower-hybrid waves in the Alcator-A tokamak shows that the fluctuation level is nearly independent of the driving field phase and begins to saturate near an incident power density of 3.5 kW/cm^2 . The waves are spread throughout the minor cross section of the plasma, have a

frequency width of 0.5 to 6 MHz about the driving frequency, and are consistent with a broad N_{\parallel} spectrum ranging from 2.5 to 6.

We wish to acknowledge the support of the Alcator group and in particular to thank S. A. Fairfax, B. R. Kusse, and M. Porkolab for their part in the design and fabrication of the lower-hybrid experiment. The Alcator Project is supported by the U. S. Department of Energy Grant No. EG-78-C-3109. We also wish to acknowledge the extensive assistance of D. Perry and useful conversations with E. Ott, R. J. Peyton, and M. Porkolab.

^(a)Visiting scientist, Francis Bitter National Magnet Laboratory, Massachusetts Institute of Technology, Cambridge, Mass. 02139.

¹R. E. Slusher and C. M. Surko, *Phys. Rev. Lett.* **40**, 400, 593(E) (1978), and references therein.

²J. J. Schuss, S. A. Fairfax, B. R. Kusse, R. R. Parker, M. Porkolab, D. Gwinn, I. Hutchinson, D. Overskei, D. Pappas, L. Scaturro, and S. Wolfe, to be published.

³M. Brambilla, *Nucl. Fusion* **16**, 47 (1976), and private communication.

⁴V. Krapchev and A. Bers, *Nucl. Fusion* **18**, 519 (1978).

⁵See, for example, P. M. Bellan and M. Porkolab, *Phys. Fluids* **19**, 955 (1976).

⁶C. M. Surko and R. E. Slusher, *Phys. Rev. Lett.* **37**, 1747 (1976).

⁷P. M. Bellan and K. L. Wong, *Phys. Fluids* **21**, 592 (1978); R. L. Berger, L. Chen, P. K. Kaw, and F. W. Perkins, *Phys. Fluids* **20**, 1864 (1977); A. Sen and N. J. Fisch, *Bull. Am. Phys. Soc.* **23**, 789 (1978), and to be published; E. Ott and R. V. Lovelace, *Bull. Am. Phys. Soc.* **23**, 765 (1978).

⁸E. Ott, to be published.

Guiding-Center Hamiltonian for Arbitrary Gyration

Harry E. Mynick^(a)

Lawrence Berkeley Laboratory, University of California, Berkeley, California 94720

(Received 2 April 1979)

A systematic procedure for deriving the guiding-center Hamiltonian K is described, valid for arbitrary ratio of particle gyro-scale length to perpendicular magnetic scale length. Practical examples are given where the method permits an explicit evaluation of K for cases where the small-gyroradius approximation used for standard guiding-center theories is invalid.

Standard guiding-center theory assumes that a particle's gyro-orbit is well approximated by a circle, centered about a particular magnetic field line. In addition, it is assumed that the param-

eter η (the ratio of the radius ρ of the gyro-orbit to the magnetic scale length L_{\perp} normal to the magnetic field \vec{B}) is small enough that the particle motion may be described in terms of \vec{B} and